

# Kinetic Monte Carlo simulations of plasma-surface reactions on heterogeneous surfaces

Daniil Marinov (✉)

IMEC, 3001 Leuven, Belgium

© Higher Education Press and Springer-Verlag GmbH Germany, part of Springer Nature 2019

**Abstract** Reactions of atoms and molecules on chamber walls in contact with low temperature plasmas are important in various technological applications. Plasma-surface interactions are complex and relatively poorly understood. Experiments performed over the last decade by several groups prove that interactions of reactive species with relevant plasma-facing materials are characterized by distributions of adsorption energy and reactivity. In this paper, we develop a kinetic Monte Carlo (KMC) model that can effectively handle chemical kinetics on such heterogenous surfaces. Using this model, we analyse published adsorption-desorption kinetics of chlorine molecules and recombination of oxygen atoms on rotating substrates as a test case for the KMC model.

**Keywords** plasma-surface interaction, kinetic Monte Carlo, plasma nano technology

## 1 Introduction

Surface processes play a central role in multiple technological applications of low temperature plasmas such as etching [1–4], deposition [5–10] and plasma catalysis [11,12]. Modelling of plasma surface interactions is essential for fundamental understanding of underlying reaction mechanisms as well as for optimization of industrial processes. However, the time and length scales involved (spanning from the atomistic to the macroscale [13]) represent a real challenge for the modelling.

Numerical simulations of plasma-surface interactions range from atomic-scale density functional theory (DFT) [14] and molecular dynamics [15] to coarse-grained deterministic and kinetic Monte Carlo (KMC) models [16]. As discussed in [16–18], KMC methods are intended

to bridge the gap between atomistic simulations and mesoscopic models. Instead of simulating exact trajectories of all atoms in the system, in KMC models, individual surface processes are treated as discrete jumps between successive states of the system. This allows one to follow the evolution of relatively large systems (typically,  $10^7$ – $10^8$  particles) on time scales ranging from nanoseconds to minutes. KMC simulations describe the statistics of elementary processes instead of calculating the exact times of occurrence of individual events. Therefore, the various processes (e.g., adsorption, desorption, diffusion, recombination, etc.) are characterized by reaction rate constants,  $r_i$ , that define the number of reaction events (equal to  $r_i \cdot \Delta t$ ) that take place on average during a time interval  $\Delta t$ . These rate constants are input parameters to KMC models and they can be either obtained by *ab-initio* calculations [14,19–21] or determined experimentally [22–28]. It should be acknowledged that KMC models lack a truly predictive power because they rely on a large number of input parameters (e.g., reaction barriers, surface densities of active sites, etc). Missing or unknown parameters may lead to inaccurate model predictions. That is why benchmarking of KMC simulations against experimental data is essential.

Most models of surface reactivity in plasmas consider homogeneous (uniform) surfaces covered with different types of active sites [29,30]. It is also assumed that all active sites of one type (e.g., chemisorption sites) are identical and can be described by a single reaction rate constant. However, it has been demonstrated experimentally by several groups that species adsorbed on real disordered plasma-facing surfaces are characterized by distributions of adsorption energy and reactivity [23,26,28,31]. In case of a discrete distribution with a small number of different types of active sites, the modelling is still straightforward [32] and can be achieved as an extension of basic models [26]. However, real surfaces are more likely to exhibit continuous distributions of parameters. For instance, spinning-wall experiments of

Received August 31, 2018; accepted March 4, 2019

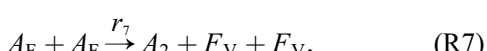
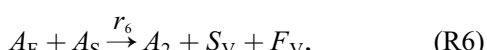
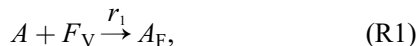
E-mail: marinov.daniil@gmail.com

Donnelly et al. [23] showed that interaction of atoms and molecules with typical reactor wall materials (i.e., Al<sub>2</sub>O<sub>3</sub>, SiO<sub>2</sub>) is characterized by broad Gaussian distributions of adsorption energy.

In this paper, we demonstrate that modelling of surface phenomena in such complex heterogeneous systems can be efficiently handled using the KMC framework. Moreover, by carefully analysing experimental results of Donnelly et al. [23] we propose an alternative interpretation of spinning-wall measurements of atomic oxygen recombination on silica. We postulate that O<sub>2</sub> molecules formed by recombination of two oxygen atoms are not instantly desorbed from the surface. Instead, the desorption occurs on the time-scale of several milliseconds giving raise to delayed desorption fluxes of O<sub>2</sub>; the distribution of adsorption energies of O<sub>2</sub> translates into the spectrum of characteristic desorption times observed in the experiments [23]. This is different from the interpretation proposed by Donnelly et al. [23] that links O<sub>2</sub> desorption with the delayed Langmuir-Hinshelwood recombination of O atoms.

## 2 KMC model formulation

KMC description is based upon a set of elementary surface processes of adsorption, desorption, diffusion, recombination, etc. In the following, we denote  $A$  ( $A_2$ ) a gas phase atom (molecule),  $F_V$  and  $S_V$  vacant physisorption and chemisorption sites, respectively,  $A_F$  and  $A_S$  a physisorbed and a chemisorbed atom. The processes of physisorption (R1), thermal desorption from physisorption sites (R2), chemisorption (R3), Eley-Rideal (E-R) recombination (R4), chemisorption via surface diffusion of physisorbed atoms (R5), Langmuir-Hinshelwood (L-H) recombination between a physisorbed and a chemisorbed atom (R6), and L-H recombination between two physisorbed atoms (R7) can be written as follows:



Processes (R1)–(R7) constitute an adequate reaction set for description of chemical kinetics on surfaces under plasma exposure. Analytical expressions for reaction rates  $r_1$ – $r_7$  as a function of input surface parameters were carefully derived and discussed in [16,30]. These reaction rates govern the KMC event selection procedure as discussed below. One should note that the set of input surface parameters determines the accuracy of KMC models and it should be examined carefully for each studied gas-solid system.

In general, KMC methods are developed to numerically solve the master equation that describes the time evolution of the system:

$$\frac{\partial P(\sigma,t)}{\partial t} = \sum_{\sigma'} [W(\sigma' \rightarrow \sigma)P(\sigma',t) - W(\sigma \rightarrow \sigma')P(\sigma,t)]. \quad (1)$$

Here,  $P(\sigma,t)$  is the probability to find the system in state  $\sigma$  at time  $t$ ,  $\sigma$  and  $\sigma'$  are two successive states of the system and  $W(\sigma' \rightarrow \sigma)$  is the probability per unit time that the system will undergo a transition from state  $\sigma'$  to state  $\sigma$ . Eq. (1) describes the increase in  $P(\sigma,t)$  due to transitions from any other state  $\sigma'$  and the decrease in  $P(\sigma,t)$  due to all transitions leaving the state  $\sigma$ . One of the major assumptions behind Eq. (1) is that the time evolution of the system is a Markov process, i.e., transition probabilities depend only on the current state of the system and not on its history.

On-lattice KMC models treat the surface as a grid of active sites where atoms and molecules can undergo adsorption, desorption, diffusion and chemical reactions. Therefore, the state of the system can be represented as a list of all active sites and adsorbed species in the simulation domain. The time evolution of the system is driven by elementary acts of adsorption, desorption, diffusion, recombination, etc. Instead of explicitly solving the master Eq. (1), KMC algorithms numerically simulate the underlying Markov process by choosing randomly among the various possible transition events and propagating the state of the system according to the selected process. At every Monte Carlo step, the time increment is calculated and the physical time is advanced.

Regardless of a particular realization, all KMC algorithms share similar features. Generally, one can consider a system that can undergo  $k$  transition events

$$E = \{e_1, e_2, \dots, e_k\}, \quad (2)$$

characterized by transition rates,

$$R = \{r_1, r_2, \dots, r_k\}, \quad (3)$$

while the number particle capable of experiencing a given event is divided as

$$N = \{n_1, n_2, \dots, n_k\}. \quad (4)$$

At each simulation step, a process and a particle have to be selected and the physical time is then advanced by generating a time increment  $\tau$

$$\tau = \frac{1}{\lambda} \ln \left( \frac{1}{u} \right), \quad (5)$$

where  $u$  is a random number drawn from uniform distribution in the unit interval [33] and

$$\lambda = \sum_i n_i r_i = \sum_i \lambda_i. \quad (6)$$

For a given gas-lattice system, different algorithms can be used to run KMC simulations leading to generally identical results [16,18,33]. Numerical efficiency and ease of implementation are the main criteria for selection of a particular KMC implementation. In [16,17], it was shown that n-fold way/Bortz-Kalos-Lebowitz (BKL) scheme is particularly suitable for simulating surface kinetics in plasmas. Algorithmically this scheme can be described as follows [16]: (i) specify simulation parameters and set the initial surface conditions at  $t = 0$ ; (ii) choose the reaction event type; (iii) choose randomly one site from the list of sites where this event can take place; (iv) execute the process and update the lattice, the reaction rates and the lists; (v) propagate the physical time by an increment calculated using equation (5); (vi) repeat until the desired physical time is reached. BKL scheme requires keeping and updating lists of active sites where particular reactions can take place in order to execute the site selection step (iii). Effective handling of these lists is essential for successful implementation of this algorithm.

In the implementation of BKL scheme discussed above, it is assumed that the surface is uniform and all active sites of the same type have identical characteristics. Here, we formulate a more general approach to simulate kinetics on surfaces with arbitrary distributions of parameters. For simplicity, we consider adsorption-desorption kinetics in a system with only one type of adsorption sites assuming a distribution of binding energy of adsorbed species. An example of such system is  $\text{Cl}_2$  interacting with the rotating substrate in the spinning wall experiment [23].

This simple system can be described by a set of two processes, adsorption (R1) and desorption (R2). The main difference in comparison to uniform surfaces is that different sites have different rate of desorption. Now, when the desorption processes is selected in the KMC scheme the site where the desorption takes place cannot be randomly picked from the list of all occupied sites. Obviously, sites with a higher desorption rate should be selected with a higher probability. The site selection procedure for non-uniform surfaces is based on the individual site-specific desorption rates  $r_2^l$  as discussed in [16]. Briefly, an array of partial sums  $s_j = \sum_{l=0}^j r_2^l / \sum_{l=0}^m r_2^l$  has to be calculated for  $1 \leq j \leq m$ , where  $m$  is the total number of occupied sites in the simulation domain.

Then, the site where the desorption takes place is selected by drawing a random number  $r$  from a uniform distribution on  $(0,1)$  and the site index  $j$  is found so that the inequality  $s_{j-1} < r \leq s_j$  is satisfied. The described approach can be extended to simulate more complex systems with multiple processes affected by distributions of surface properties. It can handle arbitrary and even time-dependent distributions.

### 3 Results and discussion

#### 3.1 Adsorption-desorption of $\text{Cl}_2$ on $\text{Al}_2\text{O}_3$ spinning wall

Here, we apply the described KMC framework to simulate adsorption-desorption kinetics of  $\text{Cl}_2$  on anodized alumina substrate that was investigated with the spinning wall method in [23]. With this technique a small cylindrical section of the reactor wall is rotated with a high speed up to 50000 r/min. The rotating surface is periodically exposed to the processing conditions and to the analysis chamber equipped with gas phase and surface diagnostics. The delay between the exposure and the analysis is varied by adjusting the rotation speed and can be reduced below 1 ms which is close to the characteristic time scales of surface reactions. Figure 1 shows desorption fluxes of  $\text{Cl}_2$  measured at different chlorine gas pressures (with plasma off) as a function of the rotation delay time between the process chamber and the analysis chamber. One can see that the desorption flux is not following a monoexponential decay which indicates the presence of a distribution of adsorption energies of  $\text{Cl}_2$  on  $\text{Al}_2\text{O}_3$ .

In the KMC model of  $\text{Cl}_2$  adsorption/desorption on the rotating substrate, surface parameters from [23] were used in simulations. The distribution of  $\text{Cl}_2$  adsorption energies was assumed to be Gaussian with the average adsorption energy of 0.56 eV and the full width at half maxima (FWHM) of 0.21 eV as depicted in Fig. 2. The total density of adsorption sites was set to  $10^{15} \text{ cm}^{-2}$  and the sticking coefficient of  $\text{Cl}_2$  was assumed to be 0.0014. With this, KMC simulations (depicted by solid lines in Fig. 1) match very well the experimental results in the whole range of gas pressures investigated in the experiment.

One should note that the experimental desorption curves shown in Fig. 1 provide information only about a limited part of the spectrum of adsorbed  $\text{Cl}_2$ . Species with low binding energies leave the surface too fast and don't contribute to the desorption flux measured in the analysis chamber. Similarly, species with high binding energies make a negligible contribution to the desorption flux. In Fig. 2, the assumed Gaussian distribution is depicted together with the characteristic desorption time at 300 K as a function of the binding energy calculated as [30]

$$\tau_d = 10^{-13} \exp(E_d/kT), \quad (7)$$

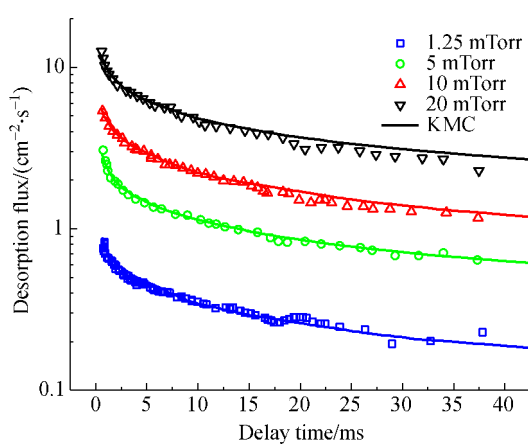


**Fig. 1** Desorption flux of  $\text{Cl}_2$  from rotating anodized alumina substrate as a function of the rotation (delay) time. Experimental data from [23] measured at different  $\text{Cl}_2$  gas pressures are depicted with open symbols. Results of KMC simulations are shown with solid lines.

where  $E_d$  is the binding energy and  $T$  is the temperature of the surface. The hatched area on the graph indicates the range of characteristic desorption times (between 0.5 and 100 ms) that can be detected in the spinning wall experiment. Therefore, Fig. 2 clearly indicates that only a part of the assumed distribution (highlighted in red) contributes to the calculated and measured desorption fluxes. Points outside of the highlighted area are not significant in the range of the characteristic desorption times covered in the experiment.

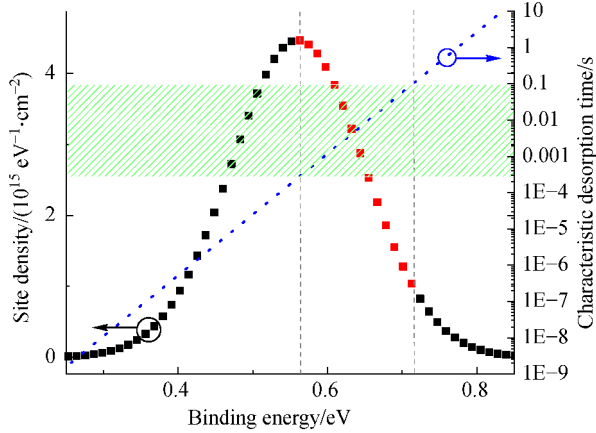


**Fig. 2** Assumed Gaussian distribution of adsorption site density over binding energy (left y-axis) and the corresponding characteristic desorption time as a function of the binding energy (right y-axis). The hatched area indicates the interval of characteristic desorption times that can be covered by the spinning wall technique. The part of the distribution that contributes to experimentally measured desorption fluxes is highlighted in red.

### 3.2 Recombination of O atoms on silica

In this section, we use KMC to investigate recombination of atomic oxygen on silica surfaces. Recombination of two oxygen atoms into a parent oxygen molecule is probably one of the most studied surface reactions both experimentally and in simulations. Nevertheless, the results of spinning wall experiments [23,31,34–36] bring new insights about the mechanisms of O recombination on surfaces that, as we show below, need to be conciliated with the existing understanding of this simple reaction.

Unlike chlorine, oxygen molecules do not stick to  $\text{SiO}_2$ -coated rotating substrates. Therefore, no  $\text{O}_2$  desorption signals (similar to those shown in Fig. 1) could be detected with plasma off. With the plasma switched on, delayed desorption of  $\text{O}_2$  from the rotating substrate was measured in the analysis chamber [31] as depicted in Fig. 3. In [31,34], this desorption flux is attributed to Langmuir-Hinshelwood recombination of oxygen atoms. In other words, it is assumed that mobile oxygen atoms can diffuse along the surface during several milliseconds after plasma exposure and eventually recombine into  $\text{O}_2$  molecules that are released into the gas phase and detected by the mass spectrometer. Therefore, the decay of the desorption flux shown in Fig. 3 is related to the lifetime of mobile oxygen atoms.

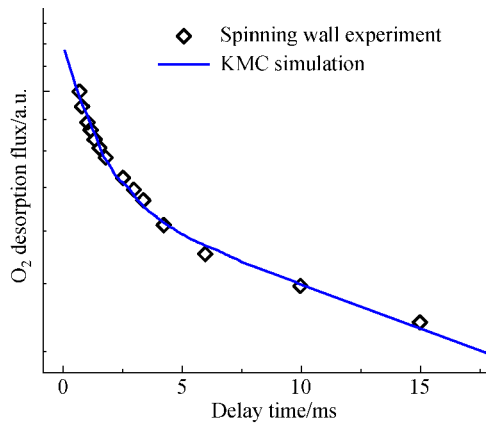
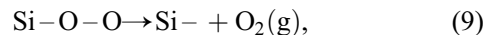
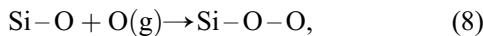


**Fig. 3** Desorption flux of  $\text{O}_2$  formed by recombination of oxygen atoms on silica-coated rotating substrate. Experimental data are taken from [31],  $p_{\text{O}_2} = 1.5$  mTorr, 400 W plasma power. KMC simulations were performed assuming the delayed desorption mechanism with two types of active sites (with  $\text{O}_2$  desorption energies 0.798 and 0.715 eV).

In conventional models of atomic recombination on surfaces [16,29,30], mobile species are associated with physisorbed atoms. The lifetime of physisorbed atoms is limited by thermal desorption and does not exceed  $10^{-8}$  s at room temperature [16]. If one assumes in simulations the lifetime of physisorbed oxygen atoms to be of the order of 10 ms (as in the spinning wall experiment) this would lead to totally unrealistic results. With this assumption, the

calculated value of the recombination probability  $\gamma_O$  is close to 1 while experimentally measured recombination probabilities on silica are much lower, typically between  $10^{-4}$  and  $10^{-2}$  [29]. Qualitatively, long-lived mobile atoms recombine with a 100% probability because they always find a partner for recombination before leaving the surface by desorption. One can conclude that the interpretation of the spinning wall experiments proposed by Donnelly et al. [23] is not fully compatible with the existing kinetic models of O recombination on silica surfaces. From the other hand, these classical models are not able to explain experimentally observed delayed desorption fluxes; physisorbed atoms are too short-lived to yield  $O_2$  desorption on time scales of milliseconds.

One of the basic assumptions of the models discussed above is that  $O_2$  molecules produced by recombination reactions (R4, R6, R7) leave the surface instantly. This assumption can be justified by the strong exothermicity of the recombination process. However, recent ab-initio simulations [14,19] predict the formation of adsorbed  $O_2$  (peroxy defect) as a result of O recombination on defective  $SiO_2$  surfaces (8). Subsequent formation of gas phase  $O_2(g)$  occurs either via thermal desorption (9) or in recombination reaction (10):



Delayed release of  $O_2$  in Reactions (9) and (10) on a millisecond time scale provides an alternative interpretation of desorption fluxes measured in spinning wall experiments.

Experimental data in Fig. 3 can be fitted with a bi-exponential decay function with characteristic times  $\tau_1 = 1.3$  ms and  $\tau_2 = 27$  ms. Assuming that  $O_2$  is produced in reactions (9) and (10) this would mean that two processes with activation energies 0.798 and 0.715 eV (estimated using (7)) are involved. The activation energy of thermal desorption from peroxy sites (9) calculated in [14] is found between 2.3 and 2.9 eV while reaction (10) is predicted to occur with little or no barrier. Thus, observed desorption of  $O_2$  with activation energy 0.7–0.8 eV is not consistent with DFT simulations [14]. One possible reason for the apparent discrepancy is that in spinning wall experiments, the rotating substrate is constantly exposed to fluxes of energetic plasma species (ions, photons, electronically excited molecules). Plasma exposure may create defect sites with lower activation barriers for  $O_2$  desorption (9) that are not captured in DFT simulations. Moreover impurities sputtered from chamber walls and redeposited on the rotating substrate may act as catalytic sites for recombination. Recombination probability of O atoms on oxidized silicon  $\gamma_O = 0.04$  measured in the spinning wall

apparatus [31] is two orders of magnitude higher than  $\gamma_O$  reported in flowing afterglow experiments on silica [29]. This points towards a significantly higher density of catalytic defects in the material used in the spinning wall experiment [31].

As a matter of fact, the value of recombination probability of O atoms on nominally identical materials measured by different authors demonstrates significant scatter and depends on a number of poorly controlled parameters such as surface pre-treatment, impurities, surface roughness and ion bombardment. In this study, we do not attempt to reconcile first principle simulations with the vast body of available experimental data. The main objective is to propose a recombination mechanism that is able to explain the results of spinning wall experiments in a non-contradicting way. Therefore, we assume in the following that experimentally observed delayed desorption fluxes originate from thermal desorption of weakly adsorbed  $O_{2ads}$  ( $E_d = 0.7$ –0.8 eV) produced by surface recombination (8);  $O_{2ads}$  remain on the surface and undergo thermal desorption (9) on the timescales of milliseconds. In the following, this recombination mechanism will be referred as a “delayed desorption” model. It should be noted that similar mechanism was used by Donnelly et al. to model recombination of Cl atoms on rotating substrates [23]. The results of KMC simulations based on the delayed desorption mechanism with two types of active sites (with activation energies for desorption equal to 0.798 and 0.715 eV) is shown in Fig. 3. Very good agreement with experimental data is obtained.

Now, we need to verify that proposed model is consistent with the large body of experimental and modelling studies of O recombination on silica surfaces. We performed KMC simulations of O recombination with the standard model developed in [16] (that considers instant desorption of  $O_2$ ) and assuming the delayed desorption of  $O_{2ads}$  with two types of active sites (as in Fig. 3). In both cases, all surface parameters were kept as in [16] and the gas phase number density of oxygen atoms was assumed to be  $10^{15} \text{ cm}^{-3}$ .

Figure 4 demonstrates that both models yield similar values of  $\gamma_O$  in a broad range of conditions. The deviation between the two cases becomes noticeable at low surface temperatures below 300 K. This is caused by blocking of surface active sites by  $O_{2ads}$  due to slower desorption rates at low surface temperatures. Obviously, sites with the highest desorption energy of  $O_{2ads}$  (and hence the lowest desorption rate) become occupied more readily. In the current model, we don't include chemical reactions between  $O_{2ads}$  and oxygen atoms. Therefore, the increased coverage of  $O_{2ads}$  is equivalent to poisoning of the surface which leads to lower values of  $\gamma_O$ .

One of the possible reaction pathways between  $O_{2ads}$  and O is formation of ozone. Significant ozone production from surface recombination of oxygen atoms has been

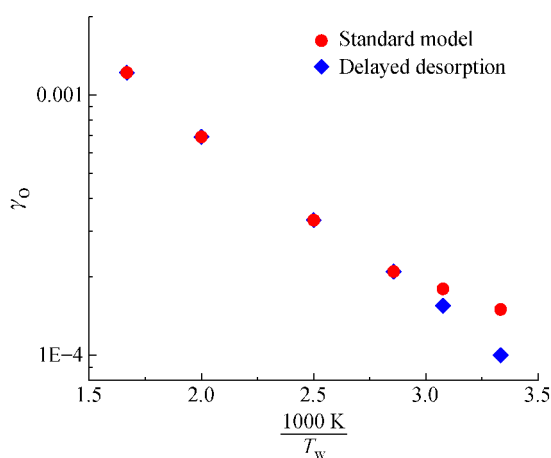


**Fig. 4** Recombination probability of atomic oxygen on silica as a function of the reciprocal substrate temperature calculated using KMC with the standard model [16] and assuming the delayed desorption mechanism with two types of active sites.

reported in [37–39]. It has been shown in [38] that ozone production accounts for up to 25% of O losses on high specific area  $\text{SiO}_2$  fibres at mbar pressures. Janssen et al. [37] reported ozone production on Pyrex with similar rate as the recombination into  $\text{O}_2$ . Regardless of its potential importance ozone production on surfaces is overlooked in kinetics models and the mechanism of this process remains poorly understood. Recombination between  $\text{O}_{2\text{ads}}$  and O is one of the possible pathways leading to the surface production of ozone. Introduction of this new  $\text{O}_3$  production mechanism in surface kinetics models and estimation of its significance is a subject for further research.

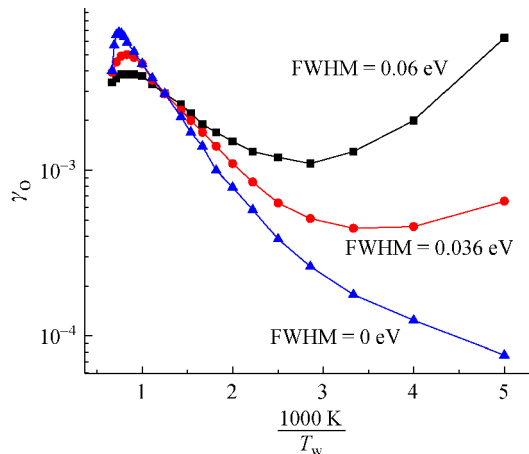
### 3.3 On the role of distributions of adsorption energy and reactivity

Previous sections clearly demonstrate that real surfaces are characterized by distributions of adsorption energy and reactivity. These distributions are not known a-priori and their experimental determination is extremely challenging. Here we use KMC framework to investigate the impact that distributions of surface properties may have on the recombination kinetics on surfaces. We assume a Gaussian distribution of adsorption energies of chemisorbed oxygen atoms on silica (as in Fig. 2),  $E_{\text{chem}}$ , with a mean value of 3.3 eV and an FWHM of 0, 0.66 and 1.1 eV. The corresponding distribution of energy barriers for recombination ( $E_R$ ) is calculated assuming  $E_R = 0.055 E_{\text{chem}}$  leading to a mean value of 0.18 eV and an FWHM 0, 0.036 and 0.06 eV, respectively. In our model, different chemisorbed atoms have different elementary probabilities of recombination with incoming oxygen atoms and, therefore, they contribute differently to the overall recombination probability. Moreover, we assume that at

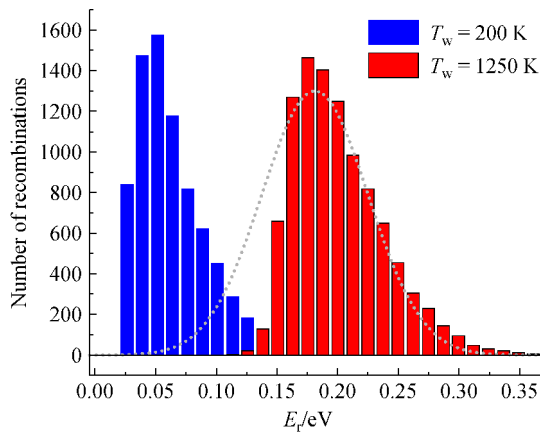
elevated temperatures chemisorbed atoms can leave the surface via thermal desorption.

Figure 5 shows calculated recombination probability  $\gamma_O$  as a function of the reciprocal surface temperature. One can note that although all assumed distributions are centered around the same mean value, the width of the distribution has a huge impact on the recombination probability in the whole range of surface temperatures. A detailed analysis shows that broader distributions lead to a higher fraction of sites featuring lower recombination barriers. Although these sites belong to the tail of the Gaussian distribution they play a very important role because of the exponential (Arrhenius) dependence of the elementary recombination probability on the value of  $E_R$ . To illustrate the contribution of these highly-reactive atoms we calculate the distribution of recombination events among different groups of atoms as a function of the corresponding value of  $E_R$  shown in Fig. 6. At low surface temperatures ( $T_w = 200$  K), the elementary recombination probability steeply decreases as the value of  $E_R$  is increased. Therefore, only atoms with low  $E_R$  in the tail of the Gaussian distribution can effectively participate in recombination. In contrast, at elevated surface temperatures ( $T_w = 1250$  K) these weakly bonded reactive atoms make no significant contribution because they quickly leave the surface via thermal desorption. Depopulation of chemisorption sites by desorption competes with the recombination processes which explains the decrease of the recombination probability in Fig. 5 at surface temperatures exceeding 1000 K.

This section illustrates the important role played by distributions of adsorption energy and reactivity in surface kinetics. Even a small fraction of highly reactive sites (i.e., chemisorbed atoms having a low energy barrier for recombination in our model) may completely dominate surface reactivity especially at low surface temperatures.



**Fig. 5** KMC calculation of recombination probability of atomic oxygen on a model surface with an assumed Gaussian distribution of energy barriers for recombination ( $E_R$ ) centered at 0.18 eV. Different curves correspond to different FWHM of the Gaussian distribution.



**Fig. 6** Distributions of recombination events among chemisorption sites caused by a distribution of energy barriers for recombination  $E_R$ . The assumed Gaussian distribution (FWHM = 0.06 eV) of surface site density over  $E_R$  is shown with a dotted line.

## 4 Conclusions

Numerous experiments unambiguously prove that surface processes on real plasma-facing materials are characterized by distributions of adsorption energy and reactivity. In this paper, we demonstrated that KMC methods are particularly suited to model surface kinetics in such complex systems on time scales relevant to real experiments which are still beyond the reach of atomistic simulations. Although KMC models rely on a large number of input parameters and lack a truly predictive power, they are a valuable tool for interpretation and analysis of plasma-surface interaction in real experimental systems.

Using the developed KMC model the results of spinning wall experiments of Donnelly et al. were analysed. We proposed an alternative “delayed desorption” mechanism to explain experimental observations of O recombination on spinning substrates and showed that this mechanism is consistent with earlier studies of O interaction with silica surfaces. Moreover, we investigated oxygen recombination on a model surface featuring a Gaussian distribution of adsorption energies of chemisorbed atoms and corresponding energy barriers for recombination. It was shown that surface kinetics is strongly influenced by the width of assumed distributions and that weakly bonded atoms dominate surface reactivity at low surface temperatures.

**Acknowledgements** Daniil Marinov has received funding from the European Union’s Horizon 2020 research and innovation programme under the Marie Skłodowska-Curie grant agreement No. 752164. DM is grateful to Prof. Vasco Guerra for fruitful discussions about surface kinetics and KMC modelling.

## References

1. Donnelly V M, Kornblit A. Plasma etching: Yesterday, today, and

- tomorrow. *Journal of Vacuum Science & Technology. A, Vacuum, Surfaces, and Films*, 2013, 31(5): 050825–050872
2. Zhang D, Kushner M J. Investigations of surface reactions during C<sub>2</sub>F<sub>6</sub> plasma etching of SiO<sub>2</sub> with equipment and feature scale models. *Journal of Vacuum Science & Technology. A, Vacuum, Surfaces, and Films*, 2001, 19(2): 524–538
  3. Brichon P, Despiau-Pujo E, Mourey O, Joubert O. Key plasma parameters for nanometric precision etching of Si films in chlorine discharges. *Journal of Applied Physics*, 2015, 118(5): 053303–053312
  4. Barone M E, Graves D B. Molecular-dynamics simulations of direct reactive ion etching of silicon by fluorine and chlorine. *Journal of Applied Physics*, 1995, 78(11): 6604–6617
  5. Benedikt J, Woen R V, van Mensfoort S L M, Perina V, Hong J, van de Sanden M C M. Plasma chemistry during the deposition of a-C:H films and its influence on film properties. *Diamond and Related Materials*, 2003, 12(2): 90–97
  6. Tsalikis D G, Baig C, Mavrantzas V G, Amanatides E, Mataras D. A hybrid kinetic Monte Carlo method for simulating silicon films grown by plasma-enhanced chemical vapor deposition. *Journal of Chemical Physics*, 2013, 139(20): 204706–204719
  7. Crose M, Sang-II Kwon J, Nayhouse M, Ni D, Christofides P D. Multiscale modeling and operation of PECVD of thin film solar cells. *Chemical Engineering Science*, 2015, 136: 50–61
  8. Zyulkov I, Krishtab M, De Gendt S, Armini S. Selective Ru ALD as a catalyst for sub-seven-nanometer bottom-up metal interconnects. *ACS Applied Materials & Interfaces*, 2017, 9(36): 31031–31041
  9. von Keudell A, Möller W. A combined plasma-surface model for the deposition of C:H films from a methane plasma. *Journal of Applied Physics*, 1994, 75(12): 7718–7727
  10. Neyts E C. PECVD growth of carbon nanotubes: From experiment to simulation. *Journal of Vacuum Science & Technology. B, Microelectronics and Nanometer Structures: Processing, Measurement, and Phenomena: An Official Journal of the American Vacuum Society*, 2012, 30: 030803–030819
  11. Neyts E C, Ostrikov K, Sunkara M K, Bogaerts A. Plasma catalysis: Synergistic effects at the nanoscale. *Chemical Reviews*, 2015, 115(24): 13408–13446
  12. Kim H H. Nonthermal plasma processing for air-pollution control: A historical review, current issues, and future prospects. *Plasma Processes and Polymers*, 2004, 1(2): 91–110
  13. Neyts E C, Bogaerts A. Understanding plasma catalysis through modelling and simulation—a review. *Journal of Physics. D, Applied Physics*, 2014, 47(22): 224010–224027
  14. Meana-Pañeda R, Paukku Y, Duanmu K, Norman P, Schwartzentruber T E, Truhlar D G. Atomic oxygen recombination at surface defects on reconstructed (0001)  $\alpha$ -quartz exposed to atomic and molecular oxygen. *Journal of Physical Chemistry C*, 2015, 119(17): 9287–9301
  15. Neyts E C, Brault P. Molecular dynamics simulations for plasma-surface interactions. *Plasma Processes and Polymers*, 2017, 14(1-2): 1600145–1600164
  16. Marinov D, Teixeira C, Guerra V. Deterministic and Monte Carlo methods for simulation of plasma-surface interactions. *Plasma Processes and Polymers*, 2017, 14(1-2): 1600175–1600192
  17. Guerra V, Marinov D. Dynamical Monte Carlo methods for plasma-

- surface reactions. *Plasma Sources Science & Technology*, 2016, 25(4): 045001–045016
- 18. Cuppen H M, Karssemeijer L J, Lamberts T. The kinetic Monte Carlo method as a way to solve the master equation for interstellar grain chemistry. *Chemical Reviews*, 2013, 113(12): 8840–8871
  - 19. Norman P, Schwartzentruber T E, Leverentz H, Luo S, Meana-Paneda R, Paukku Y, Truhlar D G. The structure of silica surfaces exposed to atomic oxygen. *Journal of Physical Chemistry C*, 2013, 117(18): 9311–9321
  - 20. Stamatakis M. Kinetic modelling of heterogeneous catalytic systems. *Journal of Physics Condensed Matter*, 2015, 27(1): 013001–013028
  - 21. Rutigliano M, Zazza C, Sanna N, Pieretti A, Mancini G, Barone V, Cacciatore M. Oxygen adsorption on  $\beta$ -cristobalite polymorph: *ab initio* modeling and semiclassical time-dependent dynamics. *Journal of Physical Chemistry A*, 2009, 113(52): 15366–15375
  - 22. Guha J, Kurunczi P, Stafford L, Donnelly V M, Pu Y K. *In-situ* surface recombination measurements of oxygen atoms on anodized aluminum in an oxygen plasma. *Journal of Physical Chemistry C*, 2008, 112(24): 8963–8968
  - 23. Donnelly V M, Guha J, Stafford L. Critical review: Plasma-surface reactions and the spinning wall method. *Journal of Vacuum Science & Technology. A, Vacuum, Surfaces, and Films*, 2011, 29(1): 010801–010825
  - 24. Guha J, Donnelly V M. Studies of chlorine-oxygen plasmas and evidence for heterogeneous formation of ClO and ClO<sub>2</sub>. *Journal of Applied Physics*, 2009, 105(11): 113307–113316
  - 25. Marinov D, Guaitella O, Rousseau A, Ionikh Y. Production of molecules on a surface under plasma exposure: Example of NO on pyrex. *Journal of Physics. D, Applied Physics*, 2010, 43(11): 115203–115209
  - 26. Guerra V, Marinov D, Guaitella O, Rousseau A. NO oxidation on plasma pretreated Pyrex: The case for a distribution of reactivity of adsorbed O atoms. *Journal of Physics. D, Applied Physics*, 2014, 47(22): 224012–224023
  - 27. Guaitella O, Lazzaroni C, Marinov D, Rousseau A. Evidence of atomic adsorption on TiO<sub>2</sub> under plasma exposure and related C<sub>2</sub>H<sub>2</sub> surface reactivity. *Applied Physics Letters*, 2010, 97(1): 011502–011504
  - 28. Marinov D, Guaitella O, de los Arcos T, von Keudell A, Rousseau A. Adsorption and reactivity of nitrogen atoms on silica surface under plasma exposure. *Journal of Physics. D, Applied Physics*, 2014, 47(47): 475204–475214
  - 29. Kim Y C, Boudart M. Recombination of oxygen, nitrogen, and hydrogen atoms on silica: Kinetics and mechanism. *Langmuir*, 1991, 7(12): 2999–3005
  - 30. Guerra V. Analytical model of heterogeneous atomic recombination on silicalike surfaces. *IEEE Transactions on Plasma Science*, 2007, 35(5): 1397–1412
  - 31. Stafford L, Guha J, Khare R, Mattei S, Boudreault O, Clain B, Donnelly V M. Experimental and modeling study of O and Cl atoms surface recombination reactions in O<sub>2</sub> and Cl<sub>2</sub> plasmas. *Pure and Applied Chemistry*, 2010, 82(6): 1301–1315
  - 32. Guerra V, Dias F M, Loureiro J, Sá P A, Supiot P, Dupret C, Popov T. Time-dependence of the electron energy distribution function in the nitrogen afterglow. *IEEE Transactions on Plasma Science*, 2003, 31(4): 542–552
  - 33. Gillespie D T. A general method for numerically simulating the stochastic time evolution of coupled chemical reactions. *Journal of Computational Physics*, 1976, 22(4): 403–434
  - 34. Kurunczi P F, Guha J, Donnelly V M. Recombination reactions of oxygen atoms on an anodized aluminum plasma reactor wall, studied by a spinning wall method. *Journal of Physical Chemistry B*, 2005, 109(44): 20989–20998
  - 35. Stafford L, Guha J, Donnelly V M. Recombination probability of oxygen atoms on dynamic stainless steel surfaces in inductively coupled O<sub>2</sub> plasmas. *Journal of Vacuum Science & Technology. A, Vacuum, Surfaces, and Films*, 2008, 26(3): 455–461
  - 36. Guha J, Khare R, Stafford L, Donnelly V M, Sirard S, Hudson E A. Effect of Cu contamination on recombination of O atoms on a plasma-oxidized silicon surface. *Journal of Applied Physics*, 2009, 105(11): 113309–113316
  - 37. Janssen C, Tuzson B. Isotope evidence for ozone formation on surfaces. *Journal of Physical Chemistry A*, 2010, 114(36): 9709–9719
  - 38. Marinov D, Guaitella O, Booth J P, Rousseau A. Direct observation of ozone formation on SiO<sub>2</sub> surfaces in O<sub>2</sub> discharges. *Journal of Physics. D, Applied Physics*, 2013, 46(3): 032001–032004
  - 39. Lopaev D V, Malykhin E M, Zyryanov S M. Surface recombination of oxygen atoms in O<sub>2</sub> plasma at increased pressure: II. Vibrational temperature and surface production of ozone. *Journal of Physics. D, Applied Physics*, 2010, 44(1): 015202–015217